INTERNATIONAL JOURNAL OF HYDROGEN ENERGY 33 (2008) 7553–7564

Available at www.sciencedirect.com

ScienceDirect

journal homepage: www.elsevier.com/locate/he

Effect of the combustion model and kinetic mechanism on the MILD combustion in an industrial burner fed with hydrogen enriched fuels

A. Parente, C. Galletti, L. Tognotti*

Dipartimento di Ingegneria Chimica, Chimica Industriale e Scienza dei Materiali, Università di Pisa, Pisa, ITALY

ARTICLE INFO

Article history:
Received 19 July 2008
Received in revised form
11 September 2008
Accepted 11 September 2008
Available online 17 November 2008

Keywords:
Flameless
Hydrogen
Combustion model
Kinetic mechanism
NOx

ABSTRACT

A numerical and experimental investigation of a burner operating in MILD combustion regime and fed with methane and methane-hydrogen mixtures (with hydrogen content up to 20% by wt.) is presented. Numerical simulations are performed with two different combustion models, i.e. the ED/FR and EDC models, and three kinetic mechanisms, i.e. global, DRM-19 and GRI-3.0. Moreover, the influence of molecular diffusion on the predictions is assessed. Results evidence the need of a detailed chemistry approach, especially with H_2, to capture the volumetric features of MILD combustion. The inclusion of molecular diffusion influences the prediction of H_2 distribution; however, the effects on the temperature field and on the major species are negligible for the present MILD combustion system. A simple NO formation mechanism based on the thermal and prompt routes is found to provide NO emissions in relatively good agreement with experimental observations only when applied on temperature fields obtained with the EDC model and detailed chemistry.

1. Introduction

Hydrogen is a promising energy carrier for the future, as, unlike electricity, it can be relatively easily stored and, unlike hydrocarbons, it does not cause any local CO_2 emission. In particular, the use of H_2-enriched fuels has received attention as such fuels may be obtained in a cheaper and ''cleaner'' manner than pure H_2, ensuring both economical and environmental benefits. For instance H_2-enriched fuels may be derived from the gasification of solid fuels, including CO_2 neutral fuels such as biomasses. Moreover H_2-enriched mixtures represent sometimes byproducts of industrial processes [1].

However, some problems arise from the utilization of such fuels as H_2 shows some specific properties (high laminar flame speed, high adiabatic flame temperature and heating value, large flammability range, high reactivity and short delay time) which make conventional burners unsuited. In fact, when operating with diffusive burners, the resulting flames are extremely stable due to the wide flammability range of H_2, but NO_x emissions are too large, because of the very high temperatures in the combustion chamber. On the other hand, premixed flames burners could prevent NO_x formation by using very lean mixtures, but this could produce stability problems and flashback phenomena. Finally, the choice of

Abbreviations: COG, coke oven gas; DO, discrete ordinates; ED, eddy dissipation model; EDC, eddy dissipation concept; FR, finite rate chemistry model; HITAC, high temperature air combustion; MD, molecular diffusion; MILD, moderate or intense low-oxygen dilution; PDF, probability density function; PSR, perfectly stirred reactor; WSGG, weighted-sum-of-grey-gases.

* Address for correspondence. Department of Chemical Engineering, Industrial Chemistry and Materials Science, University of Pisa, via Diotisalvi 2, 56126 Pisa, Italy. Tel.: +39 050 2217895; fax: +39 050 2217866.
E-mail address: alessandro.parente@ing.unipi.it (A. Parente).
0360-3199/$ – see front matter © 2008 International Association for Hydrogen Energy. Published by Elsevier Ltd. All rights reserved.
doi:10.1016/j.ijhydene.2008.09.058

Nomenclature

k	turbulent kinetic energy, $m^2\,s^{-2}$
k_R	recirculation degree
$\dot{m}_A$	air mass flow rate, $kg\,s^{-1}$
$\dot{m}_F$	fuel mass flow rate, $kg\,s^{-1}$
$\dot{m}_{EG}$	mass flow rate of recirculating exhaust gases, $kg\,s^{-1}$
$\dot{Q}_{in}$	burner input power, W
r	radial coordinate, m
T	temperature, K
$\overline{w}$	mean reaction rate, $kg\,m^{-3}\,s^{-1}$
x	axial coordinate, m
Y	mass fraction
$\tilde{Y}$	mean mass fraction
Y^*	fine structures mass fraction
Y^0	surrounding state mass fraction

Greek symbols

$\overline{\rho}$	density of the mixture, $kg\,m^{-3}$
ε_{AIR}	air excess
ε	*kinetic* energy dissipation rate, $m^2\,s^{-3}$
υ	kinematic viscosity, $m^2\,s^{-1}$
γ_λ	mass fraction of the fine structures
τ^*	mean residence time in the fine structures, s

Subscripts

k	species index
m	mixed value, referred to the mixing process of fresh and flue gases

materials becomes critical when burning H_2, because of the high temperatures reached in the combustion chamber.

Therefore, research efforts have to be spent to re-conceptualize the burner design with two main objectives: i) to upgrade conventional burners and combustion chambers for H_2-enriched fuels and ii) to design and develop new devices for pure H_2 combustion (switching from air to oxygen).

Some innovative combustion techniques have been proposed recently. Among them, flameless combustion [2] or MILD [3] or HITAC [4] is particularly appealing as it ensures high combustion efficiencies with very low pollutants emissions. MILD combustion occurs when reactants are heated above their self-ignition temperature and a strong recirculation of exhaust gases in the reaction zone lowers oxygen concentration far below the atmospheric value. The system approaches perfectly stirred reactor conditions and temperature increase due to combustion is limited to a few hundred Kelvin. Thermal NO_x formation is largely suppressed, even at the highest air preheating, because of the reduced temperature peaks.

Recently some efforts have been spent to investigate the suitability of MILD combustion with H_2-enriched fuels.

Medwell et al. [5] provided detailed measurements of temperature, OH and formaldehyde for a turbulent jet of CH_4/H_2 mixture (1/1 by vol.) in a hot and diluted coflow emulating MILD combustion conditions. The authors found that a decrease of O_2 content in the coflow leads both to a reduction of OH levels, related to the smaller temperatures, and to a broadening of the OH layer. More recently the authors extended a similar investigation to ethylene/H_2 mixtures [6].

Derudi et al. [1] used a lab-scale burner to assess the feasibility of MILD combustion for a byproduct of the coke-making process, i.e. the coke oven gas (COG), which is typically constituted by a CH_4/H_2 mixture with a composition of 40/60% by vol. The authors observed that the MILD combustion of COG requires larger jet velocity (thus larger recirculation of exhaust gases) with respect to methane; however stable MILD conditions are obtained at lower temperatures.

Sabia et al. [7] investigated the effect of H_2 addition (up to a mole fraction equal to 0.9%) on the MILD combustion of methane, by paying attention to the dynamic features of the process. The small amounts of H_2 regard its use as "fuel enhancer", to improve the characteristics of "poor" mixtures. The authors performed experiments in a jet stirred reactor, which were validated further through numerical tools for the simulation of perfectly stirred reactor conditions. The operating region of thermo-kinetics oscillations, i.e. instabilities, was found to decrease with increasing H_2 content; however the importance of irregular and double oscillations was found to increase.

Finally, it is worth mentioning that also porous radiant tube burners are being considered for the MILD combustion of H_2-enriched fuels [8], but such a technology will not be considered here as it is beyond the scope of the present work.

As emerged from the above review, most of the works on MILD combustion of H_2 containing fuels are aimed at investigating particular features and regard lab-scale devices. However, there is lack of data on practical industrial devices, which need to be upgraded to allow burning H_2-enriched fuels. Moreover, being MILD combustion profoundly influenced by fluid dynamics, it becomes crucial to analyze the specific burner conditions.

To this reason, the feasibility of MILD combustion with CH_4/H_2 mixtures in a real industrial burner is investigated both experimentally and numerically. The burner is designed to operate in MILD combustion when fed with natural gas [9]. Since the industrial characteristics of the burner prevent from carrying out a detailed and comprehensive experimental characterization, the numerical analysis plays a fundamental role in the understanding of the combustion features. Advanced numerical tools (i.e. computational fluid dynamics, CFD) are required in order to accurately describe the thermal and fluid-dynamic fields in the combustion chamber. Moreover, it is recognized that a proper choice of the physical sub-models, such as turbulence/chemistry interaction models and reaction mechanisms, is mandatory to address the complex phenomena which condition the design and upgrade of the combustion systems. Therefore, emphasis is devoted to the modeling aspect, and in particular to the effect of the combustion models and kinetic mechanisms on the temperature distribution and NO_x formation in the burner.

2. The burner

The burner is self-recuperative, with a nominal power of 13 kW [2,10]. Details of the burner may be found elsewhere [9],

however a brief description will be given in the following text for clarity of representation. A longitudinal section of the burner is reported in Fig. 1. The cylindrical combustion chamber (radius = 0.045 m, length = 0.58 m) is delimited by a radiant tube closed at the upper end. A flame tube (radius = 0.02 m, length = 0.41 m) is positioned inside the burner and promotes the internal recirculation of exhaust gases into the reaction region through three windows placed in its bottom part.

The use of such recuperative burners is widespread in the steel industry for the direct and indirect (in conjunction with radiant tubes) heating of the furnaces devoted to the steel thermal treatments, i.e. annealing process [2]. The burner under investigation represents one of the smallest cut for such heating applications, in terms of nominal input power; however it shows specific industrial features which make its experimental investigation more complicated and less controlled than for a lab-scale system.

Outside the combustion chamber, and coaxially to the radiant tube, an Inconel® shield and a water heat exchanger are placed in the experimental apparatus to replicate the real burner working conditions, ensuring heat losses towards the surroundings. Two insulation layers cover the inner and outer surfaces of the Inconel® shield, to reduce the heat transfer rate (Fig. 1). The inlet air is pre-heated by the exhaust gases in a corrugated surface heat exchanger (Fig. 1).

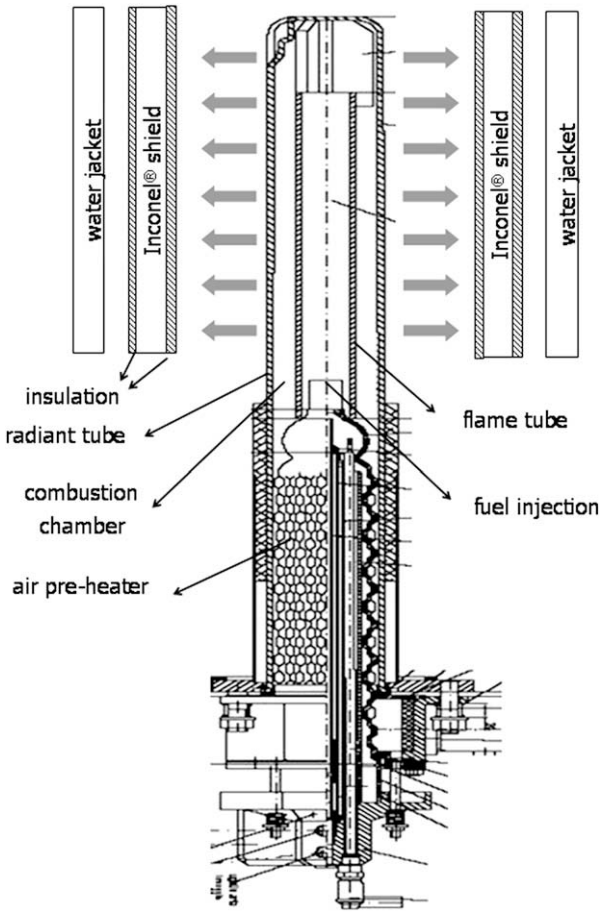

Fig. 1 – Experimental apparatus: longitudinal section of the burner and air-preheater.

Fuel and air are fed coaxially into the combustion chamber through separated jets. The fuel is fed centrally, whereas air is fed from an annular region. It is the momentum of the inlet air which drives the entrainment of exhaust gases through the recirculation windows, before reaction occurs. The burner can be characterized by a recirculation degree, k_R, defined as:

$$k_R = \frac{\dot{m}_{EG}}{(\dot{m}_F + \dot{m}_A)} \quad (1)$$

where $\dot{m}_{EG}$ is the mass flow rate of the exhaust gases recirculating into the reaction zone, whereas $\dot{m}_F$ and $\dot{m}_A$ represent the fuel and mass flow rates fed to the burner. The value of k_R was evaluated by means of the CFD simulations and it was found to be around 130% (Columns VII, Table 1). Therefore, the oxygen mass fraction in the reaction zone (after the mixing of the air and flue gases streams) was found, from the numerical simulations, to be lowered from the atmospheric value of 0.232 to about 0.12 (Column VI, Table 1), allowing the achievement of the dilution conditions which characterize the MILD combustion regime.

As far as the experimental measurements are concerned, the composition of exhaust gases are available as well as the temperatures along the radiant tube and the Inconel® shield, both of them equipped with a series of thermocouples. Unfortunately, no measurements could be made inside the burner due to its industrial characteristics. Therefore, the validation of the modeling approach is solely based on macro indicators, such as NO emissions and temperatures on the outer surface of the radiant tube, provided by the experimental campaign.

The full list of the experimental runs performed is shown in Table 1. The H_2 content of the CH_4/H_2 mixtures was increased up to 5.5% by wt. (32% by vol.).

3. Modeling approach

Numerical simulations were performed with the commercial code Fluent 6.3 by Ansys Inc. From Table 1 it can be observed that runs 1–4 were investigated both numerically and experimentally, whereas runs 5–6 were simulated only numerically, to study the effects of higher concentrations of H_2 in the fuel (up to 20% by wt.) on the results. The thermal input, Q_{in}, and air excess of runs 5–6 were set to make them directly comparable to runs 1 and 4.

The computational domain consists of a fluid domain, representing the burner interior, and two solid domains, representing the flame and radiant tubes, respectively. As mentioned in Section 2, the flame tube is equipped with three

Table 1 – Experimental and numerical runs investigated.

Run	$\dot{Q}_{in}$ [kW]	$\dot{m}_F$ [kg/s]	Y_{H_2}	ε_{AIR} [%]	$Y_{O_2,m}$	k_R [%]	CFD	Exp.
1	13.0	2.61E-04	0.000	7.0	0.118	129	X	X
2	13.0	2.50E-04	0.020	0	0.110	126	X	X
3	13.0	2.50E-04	0.041	0	0.120	130	X	X
4	13.0	2.40E-04	0.055	7.0	0.117	128	X	X
5	13.0	2.27E-04	0.100	7.0	0.118	132	X	–
6	13.0	2.01E-04	0.200	7.0	0.120	136	X	–

windows for the recirculation of exhaust gases. Therefore, a 3D model should be adopted to properly describe the recirculation process. However, in order to emphasize the role of the combustion model and kinetic mechanism on the results, a 2D computational model was adopted, to reduce the CPU time associated with the numerical simulations. The authors are aware of the error deriving from this assumption, being the recirculation degree provided a 2D model overestimated by 10–15% with respect to a 3D model [9]. However, this approximation was considered acceptable for the present study, to allow the implementation of detailed kinetic mechanisms.

A set of four 2D grids with a number of cells ranging from 15,000 to 40,000 was investigated. Although it was not possible to perform a classic Richardson extrapolation, being the grid spacing non-uniform, the values of different output variables, i.e. temperature and major species, were monitored to guide the selection of the computational grid. The selected grid is structured and non-uniform, and it consists of 19,000 hexahedrons (~316 × 60 volumes). A higher resolution was adopted in the near burner region and along the axis, to properly describe the reaction region; moreover, the air and fuel ducts were extended 50 mm upstream to ensure the flow to be fully developed at the burner exit.

As far as the boundary conditions are concerned, two user defined functions were coupled with the code in order to make the burner model self-sufficient. The air inlet temperature was evaluated as a function of the exhaust gases temperature, using an empirical correlation available from the burner supplier. Moreover, particular attention was paid to the boundary conditions of the radiant tube. As it was pointed out in Section 2, the main mode of operation of the burner is by radiation towards the surroundings. It becomes, then, crucial to properly capture the radiative heat flux emitted in order to close the energy balance in the burner. To accomplish this, the code was coupled with a subroutine for the evaluation of the heat exchange between the coaxial cylindrical shields representing the radiant tube, the internal and external insulation layers of the Inconel® shield and the water jacket. Details of the subroutine are reported in Galletti et al. [9]. The subroutine was found to perform satisfactorily, providing temperature profiles at the radiant tube catching the experimentally measured temperatures, as shown in Fig. 2.

Favre-averaged Navier–Stokes equations were solved using the standard k–ε turbulence model. The Discrete Ordinate (DO) radiation model was used with a number of directions solved equal to sixteen. The radiation properties of the reacting mixture were taken into account with the Weighted-Sum-of-Grey-Gases (WSGG) model, by using the coefficients proposed by Smith et al. [11].

Details about the turbulence/chemistry interaction models, the kinetic mechanisms and the approach used to model NO formation are given below. Also, a brief discussion regarding the approach used to account for molecular diffusion effects is provided.

3.1. *Turbulence/chemistry interaction models*

Turbulence/chemistry interactions have been modeled with two different approaches: the Eddy Dissipation/Finite Rate (ED/FR) model and the Eddy Dissipation Concept (EDC). Fast chemistry approaches (such as ED or Flamelet) were not considered as it is recognized that MILD combustion requires finite rate chemistry models [12,13].

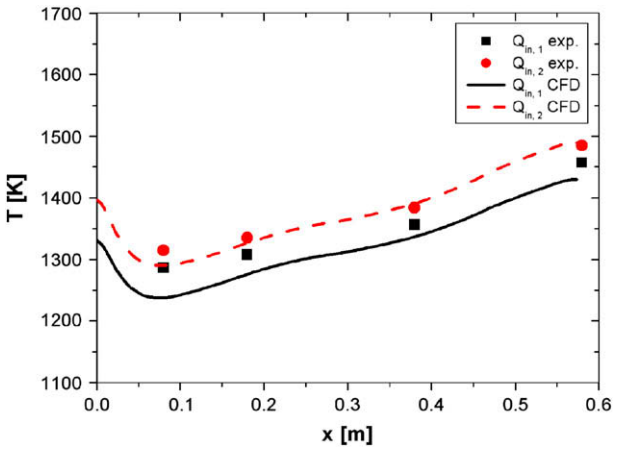

Fig. 2 – Measured and computed temperature profiles along the radiant tube for two different burner loads, i.e. $Q_{in,1}$ = 8.5 and $Q_{in,2}$ = 9.5 kW.

According to the ED/FR model both a mixing rate [14], $\overline{w}_{k,ED}$, and an Arrhenius rate, $\overline{w}_{k,FR}$, based on the mean properties, are evaluated and the smallest one is chosen as the mean reaction rate for the reacting species, i.e. $\overline{w}_k = \min(\overline{w}_{k,ED}, \overline{w}_{k,FR})$. However, the ED/FR model can handle only global kinetic mechanisms, being the turbulent rate the same for all the reactions. Therefore, if detailed chemistry is taken into account, the ED/FR model will likely produce incorrect results since the rate of production/destruction of the species has to be controlled by the Arrhenius parameters through an accurate description of turbulence/chemistry interactions. Moreover, the use of an ED/FR approach for detailed kinetic schemes could lead to numerical instabilities as it could result in sudden variations of the controlling rates within the reaction zone. Such consideration may become particularly important in MILD combustion, due to the enhanced turbulent mixing levels.

Subsequently, the Eddy Dissipation Concept (EDC) by Magnussen [15,16] was used to take into account detailed chemistry. According to EDC, combustion occurs in the regions of the flow where the dissipation of turbulent kinetic energy takes place. Such regions are denoted as fine structures and they can be described as perfectly stirred reactors (PSR). The mass fraction of the fine structures, γ_λ, and the mean residence time of the fluid within the fine structures, τ^*, are provided by an energy cascade model, which describes the energy dissipation process as a function of the characteristic scales:

$$\tau^* = 0.41\left(\frac{\nu}{\varepsilon}\right)^{1/2} \tag{2}$$

and

$$\gamma_\lambda = 2.13\left(\frac{\nu\varepsilon}{k^2}\right)^{1/4} \tag{3}$$

where ν is the kinematic viscosity and ε is the dissipation of turbulent kinetic energy, k.

The mean source term in the conservation equation for the kth species is modeled as:

$$\overline{w}_k = -\frac{\overline{\rho}\gamma_\lambda^2}{\tau^*}\frac{\left(\tilde{Y}_k - Y_k^*\right)}{\left(1-\gamma_\lambda^3\right)} \quad (4)$$

where $\overline{\rho}$ denotes the density of the mixture, Y_k^* is the mass fraction of the kth species in the fine structures and $\tilde{Y}_k$ represents the mean mass fraction of the kth species between the fine structures and the surrounding state. The value of $\tilde{Y}_k$ is obtained using:

$$\tilde{Y}_k = \gamma_\lambda^3 Y_k^* + \left(1-\gamma_\lambda^3\right)Y_k^0 \quad (5)$$

Within the context of MILD combustion, the EDC hypothesis is expected to provide satisfactory results, the system approaching perfectly stirred conditions due to the intense recirculation promoted by the internal aerodynamics. Moreover, the effect of combustion process on turbulence is expected to be less important than in a traditional flame, due to the flattening of the local temperature gradients.

3.2. *Kinetic mechanisms*

Three different kinetic mechanisms were used to describe the oxidation of methane/hydrogen mixtures. Global kinetic rates were applied with the ED/FR model for both CH_4 [17] and H_2 [18]. When using the EDC model, the global reaction approach was compared to two detailed mechanisms, the DRM-19 [20] and the GRI-3.0 [21]. The DRM-19 mechanism is a subset of the GRI-1.2 [22] full mechanism, developed to obtain the smallest set of reactions needed to reproduce closely the main combustion characteristics predicted by the full mechanism, i.e. ignition delays and laminar flame speeds. It consists of 19 species, plus Ar and N_2, for a total of 84 reversible reactions. The GRI-3.0 mechanism was implemented without the NO_x reactions, resulting in 219 reversible reactions involving 36 chemical species.

3.3. *NO modeling approach*

Thermal NO formation was modeled using a Finite Rate (FR) approach and a simplified one-step kinetic mechanism, available in the code [19] and obtained from the Zeldovich scheme by assuming a steady state for the N radicals and relating the O radical concentration to that of oxygen by means of the dissociation reaction [23]. Similarly, prompt NO formation from methane was modeled following De Soete [24]. For both thermal and prompt NO formations, the Arrhenius equation was integrated over a probability density function (PDF) for temperature in order to take into account the effect of turbulent fluctuations on the mean reaction rates [19].

3.4. *Effect of molecular diffusion*

The influence of molecular diffusion on the results was also investigated, as indicated by Christo and Dally [13]. The classical approach used in turbulent combustion modeling, which

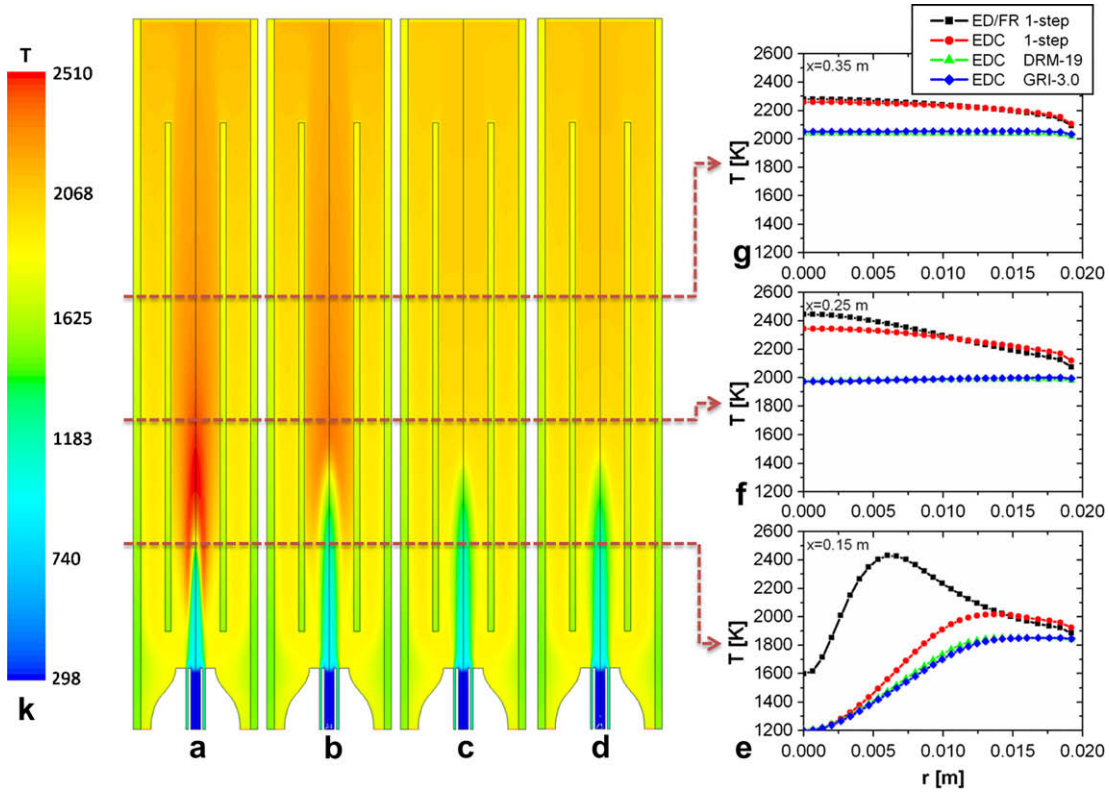

Fig. 3 – Temperature distribution in the burner fed with CH_4 (Run 1, Table 1), predicted by (a) ED/FR with global chemistry, (b) EDC with global chemistry, (c) EDC with DRM-19 and (d) EDC with GRI-3.0. Radial profiles of temperature at different axial locations along the axis, i.e. (e) $x = 0.15$ m, (f) $x = 0.25$ m, (g) $x = 0.35$ m, predicted by different combustion models and kinetic mechanisms. Burner load: 13 kW.

assumes a constant turbulent Schmidt number (equal to 0.7) and neglects the molecular contribution to the diffusion flux, was compared to the detailed specification of the laminar diffusion properties. To this purpose, the binary diffusion coefficients were calculated following the kinetic theory and a modification of the Chapman–Enskog formula [25]. Then, an effective diffusion coefficient of the species in the mixture was obtained by applying the Wilke's mixing rule [26]. The influence of molecular diffusion was investigated in the numerical simulations carried out with the EDC model and the DRM-19 kinetic mechanism.

4. Results

The results of the CFD analysis of the self-recuperative burner are presented and discussed with three main objectives: i) to investigate the effect of turbulence/chemistry interaction models and kinetic mechanism on the result, ii) to examine the effect of H_2 addition to the fuel on the temperature distributions and NO formation and iii) to assess the influence of molecular diffusion on the numerical results.

4.1. *Effect of turbulence/chemistry interaction models and kinetic mechanisms*

Fig. 3(a–d) shows the contour plot of temperature in the burner fed with CH_4 (Run 1, Table 1), obtained with different turbulence/chemistry interactions models and kinetic mechanisms. It can be observed how the ED/FR model (Fig. 3(a)) shows the presence of a lifted flame, with a well-defined high temperature region and maximum temperatures close to the adiabatic flame temperature (~2500 K). If the EDC model with global chemistry is employed (Fig. 3(b)), the resulting temperature distribution denotes an extension of the reaction zone to a larger portion of the available volume in the burner. Moreover, the "flame" appears to be more lifted, thus showing the effect of the combustion model on the ignition process. However, only when considering the DRM-19 (Fig. 3(c)) and the GRI-3.0 (Fig. 3(d)) kinetic mechanisms, a uniform temperature distribution, expected when operating in MILD combustion regime, is observed in the burner. It is also noteworthy that the results provided by the two detailed kinetic mechanisms are in very good agreement, maximum temperatures differing by just 20 K.

Such considerations can be quantitatively confirmed by the analysis of the radial profiles of temperature at different locations, x, along the burner axis (Fig. 3(e–g)). It can be observed how the ED/FR model predicts a very large temperature peak at the axial location $x = 0.15$ m (Fig. 3(e)). On the other hand, the EDC model with global chemistry provides results which do not significantly deviate from the profiles obtained with the detailed mechanisms. This result suggests that the near burner behavior is largely affected by the ability of the turbulence/chemistry interaction model to capture the ignition process. As the distance from the burner exit increases (Fig. 3(f, g)), the influence of the kinetic mechanisms

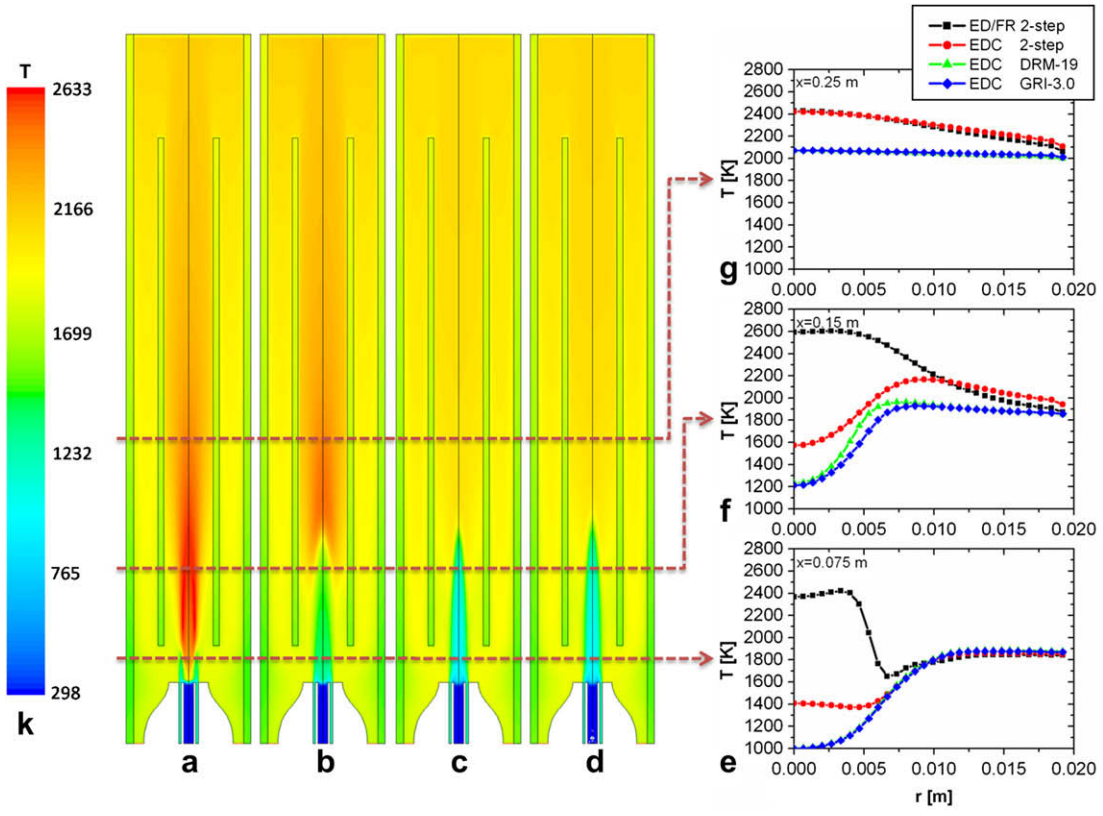

Fig. 4 – Temperature distribution in the burner fed with CH_4/H_2 (Run 4, Table 1) predicted by (a) ED/FR with global chemistry, (b) EDC with global chemistry, (c) EDC with DRM-19 and (d) EDC with GRI-3.0. Radial profiles of temperature at different axial locations along the axis, i.e. (e) $x = 0.075$ m, (f) $x = 0.15$ m, (g) $x = 0.25$ m, predicted by different combustion models and kinetic mechanisms. Burner load: 13 kW. H_2 mass fraction in the fuel: 5.5%.

on the heat release and, hence, on the temperature distribution becomes significant, leading to the overlap of the profiles provided by the ED/FR and EDC models with global chemistry. Regarding the detailed kinetic mechanisms, the DRM-19 and GRI-3.0 mechanisms are almost collapsed onto a single line and provide a homogeneous temperature distribution in the burner, without local peaks.

Fig. 4(a–d) shows the contour plots of temperature in the burner fed with a mixture containing a H_2 mass fraction equal to 5.5% (Run 4, Table 1). In such conditions, the use of the ED/FR model (Fig. 4(a)) shows a strong influence of H_2 reactivity on the temperature distribution. The reaction zone is attached to the burner and the "flame" shape resembles that of a typical diffusion flame. If the EDC model is employed (Fig. 4(b)), the reaction zone is no longer attached to the burner but shifted downstream along the axis. Again, when the detailed kinetic mechanisms are used in conjunction with EDC (Fig. 4(c, d)), the resulting temperature distribution is more homogeneous, although the effect of H_2 reactivity is visible in the reduction of the "flame" lift-off length with respect to the CH_4 case. As for the comparison between DRM-19 and GRI-3.0, a deeper penetration of the air jet is observed with GRI-3.0, indicating that a higher reactivity is predicted by the DRM-19 mechanism.

Similarly to the methane case, a better understanding of the effect of combustion models and kinetic mechanisms can be gained when analyzing the temperature profiles at different axial locations along the axis (Fig. 4(e–g)). It can be observed how the use of the ED/FR model results in a significant temperature increase in the near burner region, at an axial distance x equal to 0.075 m (Fig. 4(e)). This behavior can be ascribed to the high reactivity of H_2 resulting from the decoupled treatment of CH_4 and H_2 oxidation processes, which leads to the early oxidation of H_2. Moreover, differently to the CH_4 case, the temperature profiles predicted by the EDC model with global chemistry significantly diverge from those obtained with the detailed kinetic mechanisms in the region close to the burner exit, thus underlying the effect of H_2 reactivity, enhanced by the global chemistry approach. Similarly to the CH_4 case, the discrepancies between the global and detailed kinetic approaches increase with the axial distance resulting in the overlap of the temperature profiles given by the ED/FR and EDC with global chemistry for $x = 0.25$ m (Fig. 4(g)). Again, it can be observed how the DRM-19 and GRI-3.0 mechanisms provide very similar results, leading to radial temperature profiles almost collapsing onto a single line. Small differences, below 10% with respect to the GRI-3.0 case, are observed at the axial location $x = 0.15$ m, indicating the earlier ignition predicted by the DRM-19 mechanism (Fig. 4(f)).

4.2. *Effect of H_2 addition to the fuel*

Fig. 5(a–d) compares the temperature distributions in the burner fed with mixtures containing mass fractions of H_2 up to 20% (Runs 1, 4–6, Table 1), obtained with the EDC

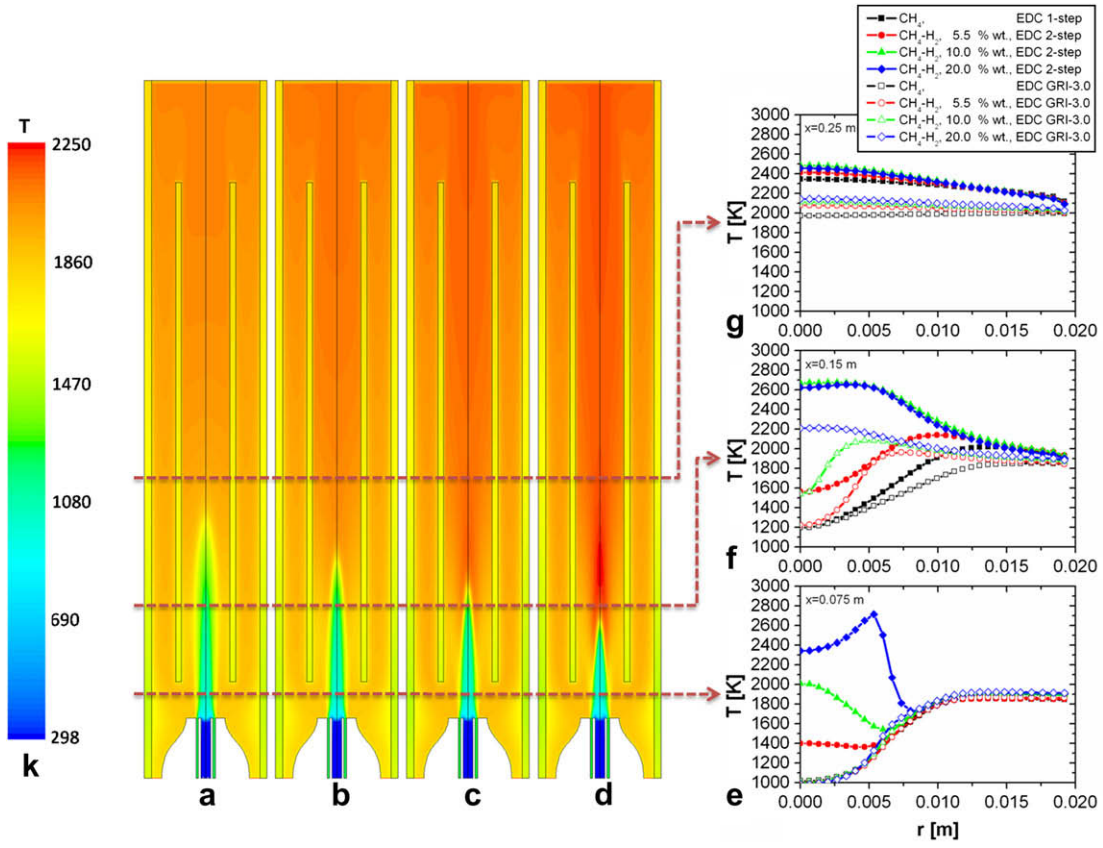

Fig. 5 – Temperature distribution predicted by EDC with GRI-3.0 in the burner fed with increasing H_2 mass fraction (Runs 1, 4–6, Table 1): (a) 0%, (b) 5.5%, (c) 10% and (d) 20%. Radial profiles of temperature at different axial locations along the axis, i.e. (e) $x = 0.075$ m, (f) $x = 0.15$ m, (g) $x = 0.25$ m, predicted by EDC with global chemistry and GRI-3.0. Burner load: 13 kW.

combustion model and the GRI-3.0 kinetic mechanism. The contour plots show that the addition of H_2 determines the increase of the temperature levels in the burner as well as the reduction of the lift-off length and the shift of the reaction zone towards the burner exit. The temperature increase is not only due to the higher specific energy content of the H_2 blended fuel with respect to methane, but also to the reduced radiation losses from the flame, determined by the decrease of CO_2 formation [27,28].

The influence of the kinetic mechanisms on the results can be assessed by comparing the radial profiles of temperature at different heights along the axis, as provided by the global and detailed chemistry approaches (Fig. 5(e–g)). It can be observed how, in the near burner region (Fig. 5(e)), the use of a global kinetic scheme determines the formation of temperature peaks which become more and more pronounced as the H_2 content in the fuel increases. Instead, when the GRI-3.0 mechanism is associated to the EDC model (Fig. 5(e)), no influence of H_2 addition on the temperature profiles is observed at the axial location $x = 0.075$ m, the temperature simply increasing from the air inlet temperature to the recirculating flue gases temperature. The effect of H_2 becomes relevant for both the kinetic mechanisms at $x = 0.15$ m (Fig. 5(f)). The radial temperature profiles show, for both cases, a generalized increase of the temperature levels in the burner when increasing the mass fraction of H_2 in the fuel stream. Moreover, H_2 addition causes the maximum temperature to shift towards the burner axis, denoting a minor penetration of the exhaust gases in the fresh mixture, due to the higher reactivity of the fuel. Such behavior can be explained by the direct effect of hydrogen on the chain carrying radicals, i.e. H, O and OH, which globally results in the enhancement of the combustion rate of methane and in the shortening of the visible flame length, as observed experimentally by Chouduri and Gollahalli [28] for turbulent jet diffusion flames.

However, it should be underlined how the detailed mechanism predicts temperature levels in the burner far below the (unrealistic) ones given by the global approach, and provides a significantly more uniform temperature distribution, as one would expect in a MILD combustion regime. With respect to the CH_4 case, the EDC with the GRI-3.0 mechanism predicts an increase of the maximum temperature in the burner by 150 K with a mass fraction of H_2 in the fuel equal to 20%, whereas the global chemistry approach would lead, in the same conditions, to an increase higher than 400 K. Such temperature increase is expected to affect dramatically the estimated NO emissions from the burner, as described in the following text. The effect of H_2 on the burner operation is also visible from the contour plots of OH radical in the burner with increasing H_2 mass fraction (Runs 1, 4–6, Table 1), obtained with the EDC model and the GRI-3.0 mechanism (Fig. 6(a–d)). It is clear how the addition of H_2 causes an increase of the OH concentration in the burner and the formation of a high reactivity core, as shown by the temperature distributions

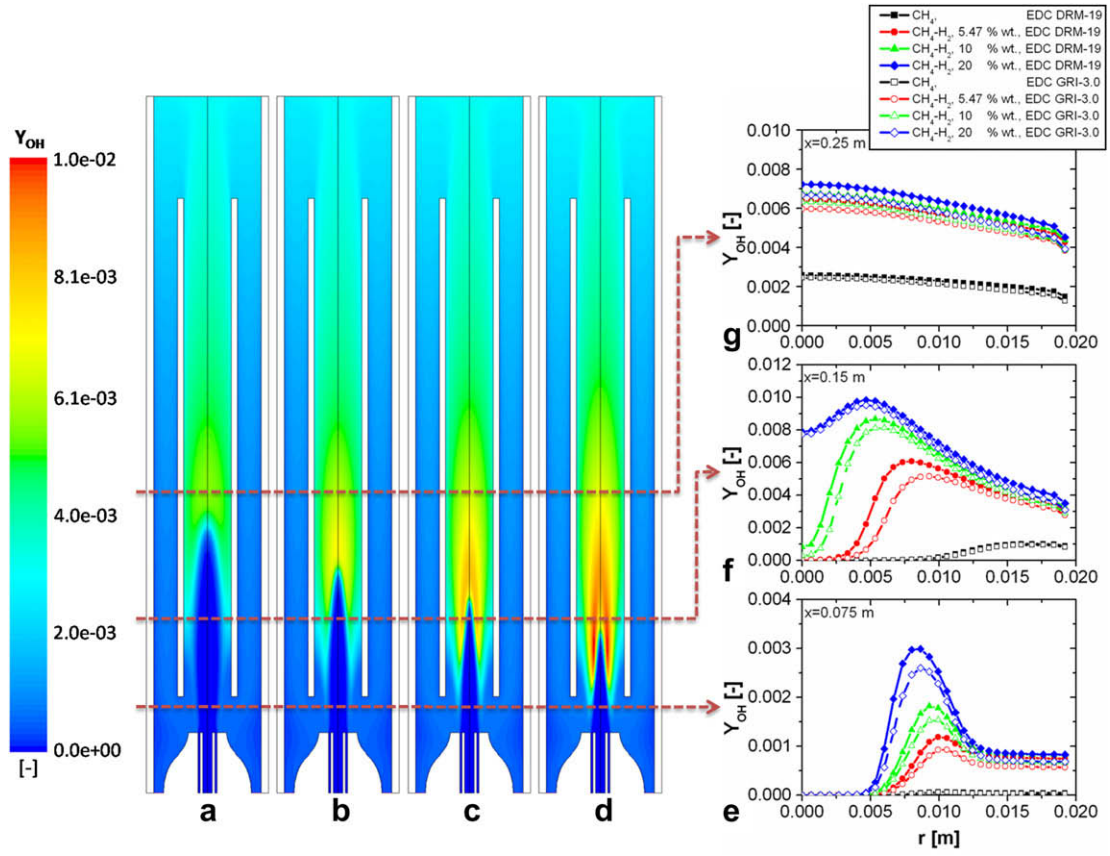

Fig. 6 – OH radical distribution predicted by EDC with GRI-3.0 in the burner fed with increasing H_2 mass fraction (Runs 1, 4–6, Table 1): (a) 0%, (b) 5.5%, (c) 10% and (d) 20%. Radial profiles of temperature at different axial locations along the axis, i.e. (e) $x = 0.075$ m, (f) $x = 0.15$ m, (g) $x = 0.25$ m, predicted by EDC with DRM-19 and GRI-3.0. Burner load: 13 kW.

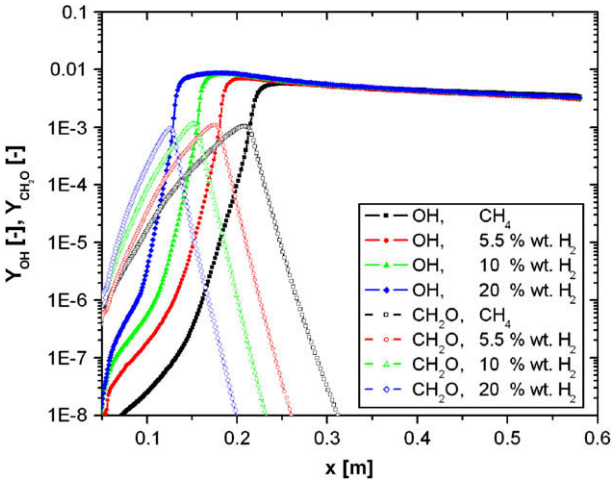

Fig. 7 – Axial profile at $r = 0$ of OH radical and CH_2O species mass fraction. Runs 1, 4–6, Table 1.

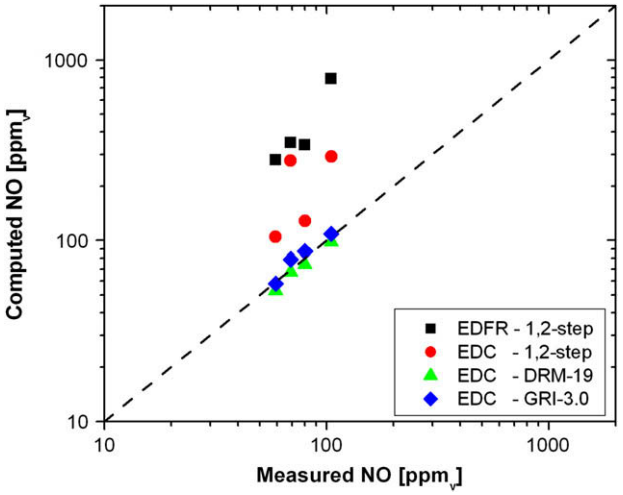

Fig. 8 – Comparison of predicted and measured NO emissions in the flue gases (Runs 1–4, Table 1).

(Fig. 5(a–d)). Moreover, the profiles of OH radical mass fraction (Fig. 6(e–g)) show a radial spread of OH when increasing the H_2 in the fuel. Such behaviour is expected, since hydrogen increases the production of OH through the chain branching reactions [29,30].

Finally, regarding the comparison between DRM-19 and GRI-3.0, the radial temperature profiles of Fig. 6(e–g) show that the two kinetic mechanisms are in good agreement, being the maximum observed differences below to 20% (with respect to the GRI-3.0 predictions). This can be considered acceptable, especially because such differences are reflected in discrepancies on the predicted temperature fields safely below 10%.

Fig. 7 shows the axial profiles of the OH radical and CH_2O intermediate species mass fractions, with a H_2 mass fraction in the fuel ranging from 0 to 20%. The figure confirms the main effect of H_2 on the "flame" structure inside the burner. When the mass fraction of H_2 is increased, the OH peak rises and shifts backward along the axis. The existence of a diffuse and extended reaction zone is confirmed by the axial profiles of OH reaching almost a plateau value. Moreover, Fig. 7 clearly indicates the role of the intermediate species CH_2O as "ignition marker", in contrast to the "flame marker" OH, as experimentally observed by Medwell et al. [5,6]. The CH_2O peak anticipates the OH maximum and indicates the attachment height of the reaction zone. Again, it can be observed how ignition occurs faster when H_2 is added to the fuel.

Table 2 lists the computed maximum temperatures in the burner and the NO emissions, predicted and measured, as a function of the H_2 content in the fuel stream. As it was pointed out in Section 2, there is no access to the burner interior. Therefore, the numerical models adopted can be assessed only through macro-indicators such as the NO emissions available in the experimental measurements. Moreover, a proper prediction of the NO trends is mandatory, being MILD combustion an appealing technology for reducing NO_x pollutants.

It can be observed (Table 2) how the maximum temperature in the burner increases with the hydrogen fraction with all the turbulence/chemistry interactions models and kinetic mechanisms used, with the exception of the case corresponding to a H_2 mass fraction equal to 2% (run 2, Table 1). However, this experimental run was performed nearly at stoichiometric conditions, thus at conditions not directly comparable to runs 1, 4–6. Table 2 also indicates that, following the maximum temperatures, also the NO emissions show a generalized increasing trend with the H_2 fraction. Considering only the experimental data, it can be observed how the measured NO emissions are almost doubled, from ~50 to ~100 ppm_v when increasing the H_2 mass fraction from 0 to 5.5%. Such an increase could be regarded as unacceptable with respect to existing environmental regulation. Then, a burner modification could be proposed, by reducing the air inlet cross sectional

Table 2 – Computed maximum temperatures and, predicted and measured, NO emissions with different combustion models and kinetic mechanisms.

Run	T_{max} [K]				NO [ppm_v]				
	ED/FR	EDC 1,2-step	EDC DRM-19	EDC GRI-3.0	ED/FR	EDC 1,2-step	EDC DRM-19	EDC GRI-3.0	Exp.
1	2510	2345	2082	2100	348	276	67	79	69
2	2488	2324	2092	2107	280	105	53	58	59
3	2558	2377	2115	2132	337	128	74	87	80
4	2635	2492	2114	2130	786	291	98	109	105
5	2690	2710	2170	2160	1266	1244	136	158	–
6	2720	2765	2243	2250	1655	1810	165	192	–

area in order to enhance the recirculation of exhaust gases in the reaction zone and the dilution effects on the reacting mixture [9]. Finally, Table 2 underlines that the EDC model with global chemistry results in higher temperatures and, consequently NO levels with respect to ED/FR, when the H_2 mass fraction in the fuel is higher than 5.5%.

The comparison between the predicted and measured NO emissions (columns VI–X, Table 2) is shown graphically in Fig. 8. It can be clearly observed how it is possible to get close to the experimental measurements only by using an accurate description of turbulence-chemistry interactions and chemical kinetics. In all cases, the ED/FR and EDC models with global chemistry lead to a significant overprediction of the NO emissions. For instance, when using the EDC model, the NO emissions estimated for the CH_4 case using the temperature field given by the global kinetic mechanism were about 350 ppm_v, thus much larger than those obtained from the temperature field provided by the DRM-19 and GRI-3.0, i.e. ~70 and ~80 ppm_v (the NO measured value was 79 ppm_v). This effect becomes more pronounced when H_2 is added to the fuel. For a H_2 mass fraction of 20%, NO emissions of about 1810 ppm_v were obtained using global chemistry, whereas NO emissions of about 165 and 190 ppm_v were obtained from the temperature distributions provided by the DRM-19 and GRI-3.0 mechanisms, respectively.

Fig. 8 seems to suggest that better predictions can be achieved with the DRM-19 mechanism. However, it is not possible to derive any conclusion from the observed behavior as this

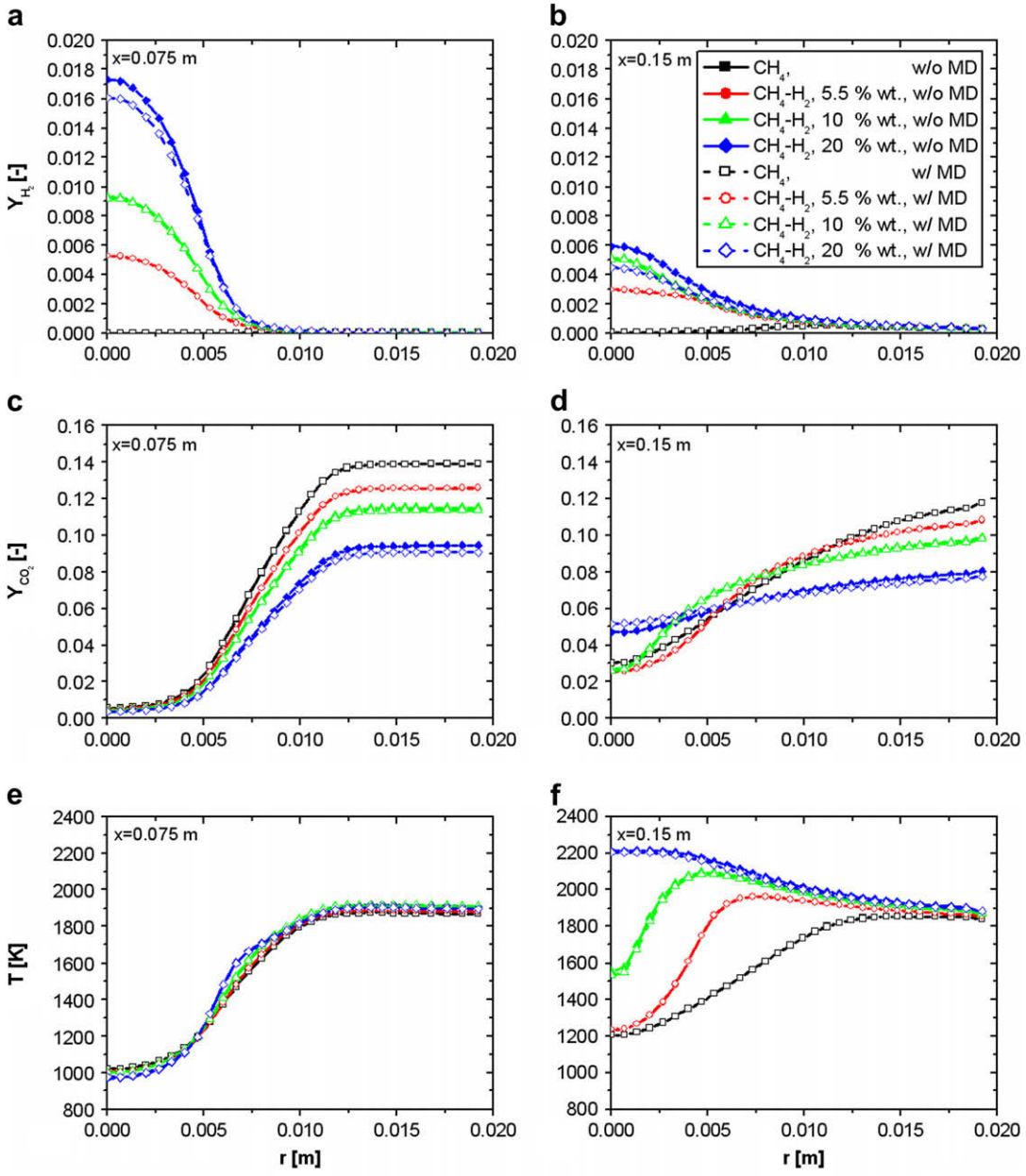

Fig. 9 – Effect of molecular diffusion on the radial profiles of (a, b) H_2 mass fraction, (c, d) CO_2 mass fraction and (e, f) temperature at different axial locations along the burner axis. Combustion model and kinetic mechanism: EDC with DRM-19. Runs 1, 4–6, Table 1.

could be imputed to the overestimation of the NO rates determined by the simplified NO formation mechanism adopted.

Concluding, the analysis of the computational results and their comparison to the experimental data suggest that the conditions of uniform temperature distribution, characteristic of the MILD combustion regime, allow capturing NO trends even with a simplified NO formation model, as the one used in the present work, given an adequate characterization of the temperature distribution in the burner. Obviously, the prerequisite for the validity of such a result is that the NO formation is dominated by the thermal mechanism and that the temperature is almost uniform inside the burner. However, MILD combustion typically occurs at lower temperatures so that other mechanisms, such as the N_2O route, may become dominant [31]. Moreover, when hydrogen is added to the fuel, the NNH path may play a significant role [32]. In such cases the simple NO formation approach adopted in the present study could be inadequate and other solutions, as CFD kinetic post-processing techniques [33] could be considered. Anyhow, a good estimation of the temperature field through a proper choice of kinetic mechanisms and combustion models represents a fundamental prerequisite, as it is addressed in the present study.

4.3. *Effect of molecular diffusion*

Fig. 9 shows the effect of molecular diffusion on the (a, b) H_2, (c, d) CO_2 and (e, f) temperature radial profiles at two different axial locations along the axis. It can be observed (Fig. 9(a, b)) that the laminar diffusion has some influences on the H_2 distribution in the burner, when the H_2 content in the fuel is higher than 10%. The maximum difference between the radial profiles obtained with and without differential diffusion effects are observed at the axial location $x = 0.15$ m and are of the order of 15%, for a H_2 mass fraction equal to 0.2. However, this affects very slightly the distribution of the major species, such as CO_2, and temperature. In fact, Fig. 9(c–f) points out how the variations in the radial profiles of CO_2 and temperature, when including the effects of molecular diffusivity, are negligible, being in all cases lower than 5%. This is in contrast to the behaviour observed by Christo and Dally [13], who found the differential diffusion to play a major role in the numerical simulation of a jet issuing in a hot diluted coflow. However, the different findings of the present study could be ascribed to the intense recirculation and to the enhanced turbulence levels in the burner, which have a direct effect on the turbulent viscosity and, therefore, on the turbulent contrbution to the diffusive flux. Such consideration was quantitatively confirmed by the analysis of the distribution of the H_2 molecular to effective diffusion ratio inside the combustion chamber. The turbulent contribution was found to be dominant in the near burner region, where the ignition process takes place, representing around 85% of the effective diffusion coefficient for the 20% hydrogen case.

5. Conclusions

A numerical and experimental investigation of a burner operating in MILD combustion regime and fed with methane and methane–hydrogen mixtures has been presented.

Results showed the major role played by the turbulence-chemistry interactions models and kinetic mechanisms in the simulation of the MILD combustion regime.

In particular, the ED/FR model was found to be unable to capture the volumetric features of MILD combustion, leading to maximum temperatures in the burner close to the adiabatic flame temperature. Similarly, the EDC model with global chemistry was found to perform unsatisfactory, being extremely sensitive to the addition of H_2 to the fuel stream and leading to temperature profiles overlapping those given by the ED/FR in the far burner region. On the other hand, the EDC with detailed chemistry provided results showing a more uniform distribution of temperature as well as the extension of the reaction zone to a large portion of the available volume in the burner, as it would be expected in a MILD combustion regime. Moreover, the temperature increase due to H_2 addition to the fuel, as provided by the detailed chemistry approach, was substantially limited with respect to the global approach, leading to a reduced increase of the NO emissions, as shown by the experimental data. On conclusion, the conditions of high dilution and enhanced mixing which characterize MILD combustion, determine the combustion and chemistry models to play a major role in the numerical modeling. In particular, the addition of hydrogen results in very complex oxidation behaviors, which need to be addressed with detailed kinetic mechanisms.

As far as the NO emissions are concerned, a rather simple mechanism based on a one-step equation integrated over a PDF of temperature, for both the prompt and thermal NO, was found to perform satisfactory when coupled with the EDC model and detailed chemistry. This is due to the relatively high temperatures which characterize the operation of the present burner and make the NO formation dominated by the thermal mechanism.

Finally, the role of the molecular diffusivity on temperature and major species distribution in the burner was found to be negligible, leading to variations below 5% in all cases, although a visible effect was observed for the distribution of highly diffusing species, such as H_2, when the H_2 mass fraction was above 10%. The results obtained are not to be considered applicable to MILD combustion in general, being strictly related to the particular burner geometry and operation which ensures the MILD regime (exhausts recirculation and oxidant dilution).

Acknowledgments

We kindly thank Dr. Schiavetti and Dr. Riccardi from ENEL for the experimental campaign.

REFERENCES

[1] Derudi M, Villani A, Rota R. Mild combustion of industrial hydrogen-containing byproducts. Ind Eng Chem Res 2007;46:6806–11.

[2] Wünning JA, Wünning JG. Flameless oxidation to reduce thermal no-formation. Prog Energy Combust Sci 1997;23:81–94.

[3] Cavaliere A, de Joannon M. Mild Combustion. Prog Energy Combust Sci 2004;30:329–66.
[4] Gupta AK. Thermal characteristics of gaseous fuel flames using high temperature air. J Eng Gas Turbines Power Transaction of ASME 2004;126:9–19.
[5] Medwell PR, Kalt PAM, Dally BB. Simultaneous imaging of OH, formaldehyde, and temperature of turbulent nonpremixed jet flames in a heated and diluted coflow. Combust Flame 2007;148:48–61.
[6] Medwell PR, Kalt PAM, Dally BB. Imaging of diluted turbulent ethylene flames stabilized on a jet in hot coflow (JHC) burner. Combust Flame 2008;152:100–13.
[7] Sabia P, de Joannon M, Fierro S, Tregrossi A, Cavaliere A. Hydrogen-enriched methane mild combustion in a well stirred reactor. Exp Therm Fluid Sci 2007;31:469–75.
[8] Gauthier SE, Lebas E, Baillis D. SFGP 2007-natural gas/hydrogen mixture combustion in a porous radiant burner. Int J Chem React Eng 2007;5:A114.
[9] Galletti C, Parente A, Tognotti L. Numerical and experimental investigation of a mild combustion burner. Combust Flame 2007;151:649–64.
[10] Gheri P, Gigliucci G, Monticelli M, Schiavetti M. Studio e sperimentazione di tecnologie flameless per la combustione dell'idrogeno: sperimentazione ed analisi modellistica del combustore flameless con miscele metano-idrogeno (in Italian). ENEL report number ENELP/RIC/PI/RT-2004/0102; 2004.
[11] Smith F, Shen ZF, Friedman JN. Evaluation of coefficients for the weighted sum of gray gases model. J Heat Transfer 1982; 104:602–8.
[12] Coelho PJ, Peters N. Numerical simulation of a mild combustion burner. Combust Flame 2001;124:503–18.
[13] Christo FC, Dally BB. Modeling turbulent reacting jets issuing into a hot and diluted coflow. Combust Flame 2005;142: 117–29.
[14] Spalding DB. Mixing and chemical reaction in steady confined turbulent flames. Proc Combust Inst 1971;13:649–57.
[15] Magnussen BF, Hjertager BH. On mathematical modeling of turbulent combustion with special emphasis on soot formation and combustion. Proc Combust Inst 1976;16: 719–29.
[16] Gran IR, Magnussen BF. A numerical study of a bluff-body stabilized diffusion flame. Part 2. Influence of combustion modeling and finite-rate chemistry. Comb Sci Technol 1996; 119:191–217.
[17] Westbrook CK, Dryer FL. Simplified reaction mechanisms for the oxidation of hydrocarbon fuels in flames. Combust Sci Technol 1981;27:31–43.
[18] Chakraborty B, Paul PJ, Mukunda HS. Evaluation of combustion models for high speed H_2/air confined mixing layer using DNS data. Combust Flame 2000;121:195–209.
[19] Fluent 6.3 User Guide.
[20] Kazakov A, Frenklach M. Reduced reaction sets based on GRI-Mech 1.2. Available at http://www.me.berkeley.edu/drm/.
[21] Smith GP, Golden DM, Frenklach M, Moriarty NW, Eiteneer B, Goldenberg M, et al. GRI-3.0. Available at http://www.me.berkeley.edu/gri_mech/.
[22] Frenklach M, Wang H, Yu C-L, Goldenberg M, Bowman CT, Hanson RK, et al. GRI-1.2. Available at http://www.me.berkeley.edu/gri_mech/.
[23] Westenberg AA. Kinetics of NO and CO in lean, premixed hydrocarbon–air flames. Combust Sci Technol 1971;4:59–64.
[24] De Soete GG. Proc Combust Inst 1974;15:1093–102.
[25] McGee HA. Molecular engineering. New York: McGraw-Hill; 1991.
[26] Wilke SP. A viscosity equation for gas mixtures. J Comput Phys 1950;18:517–9.
[27] Ilbas M. The effect of thermal radiation and radiation models on hydrogen–hydrocarbon combustion modeling. Int J Hydrogen Energy 2005;30:1113–26.
[28] Choudhuri AR, Gollahalli SR. Global characteristics of hydrogen–hydrocarbon composite fuel turbulent jet flames. Int J Hydrogen Energy 2003;28:445–54.
[29] Choudhuri R, Gollahalli SR. Intermediate radical concentrations in hydrogen–natural gas blended fuel jet flames. Int J Hydrogen Energy 2004;29:1293–302.
[30] Echekki T, Chen JH. Direct numerical simulation of autoignition in non-homogeneous hydrogen–air mixtures. Combust Flame 2003;134:169–91.
[31] Szegö GG, Dally BB, Nathan GJ. Scaling of NO_x emissions from a laboratory-scale mild combustion furnace. Combust Flame 2008;154:281–95.
[32] Skottene M, Rian KE. A study of NO_x formation in hydrogen flames. Int J Hydrogen Energy 2007;32:3572–85.
[33] Mancini M, Schwöppe P, Weber R, Orsino S. On mathematical modelling of flameless combustion. Combust Flame 2007;150:54–9.